Supplement of Atmos. Meas. Tech., 19, 7835–7852, 2026
https://doi.org/10.5194/amt-19-7835-2026-supplement
© Author(s) 2026. CC BY 4.0 License.



Atmospheric Measurement Techniques
Open Access
EGU

Supplement of

Propagation of CAMS aerosol uncertainty to clear-sky solar irradiance estimates

Anna Moustaka et al.

Correspondence to: Anna Moustaka (anna.moustaka@pmodwrc.ch)

The copyright of individual parts of the supplement might differ from the article licence.

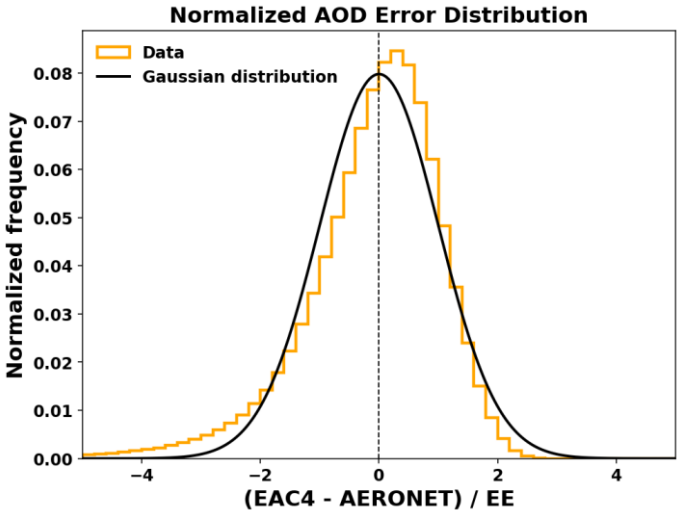


Figure S1: Histogram of the normalized AOD retrieval errors, defined as $AOD_{EAC4} - AOD_{AERONET}/EE$, for all collocated EAC4–AERONET observations used in the uncertainty analysis. The orange histogram represents the normalized frequency distribution of the retrieval differences, while the black curve corresponds to an idealized Gaussian distribution with zero mean and unit variance, $\mathcal{N}(0, 1)$.

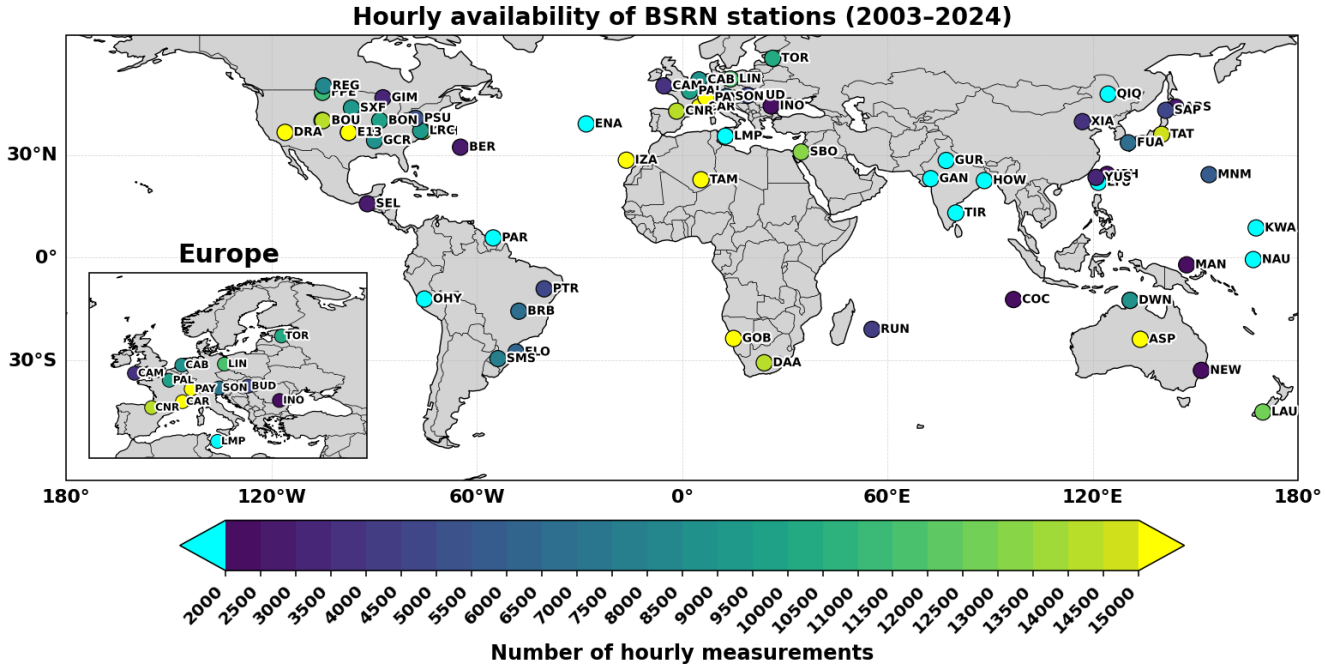


Figure S2: Spatial distribution of the 64 BSRN stations retained for the validation of the EAC4-derived irradiance products (i.e., GHI and DNI) after applying all quality-control criteria. The color scale indicates the number of hourly measurements available at each station during the 2003–2024 period. The inset axis highlights the station spatial distribution over Europe.

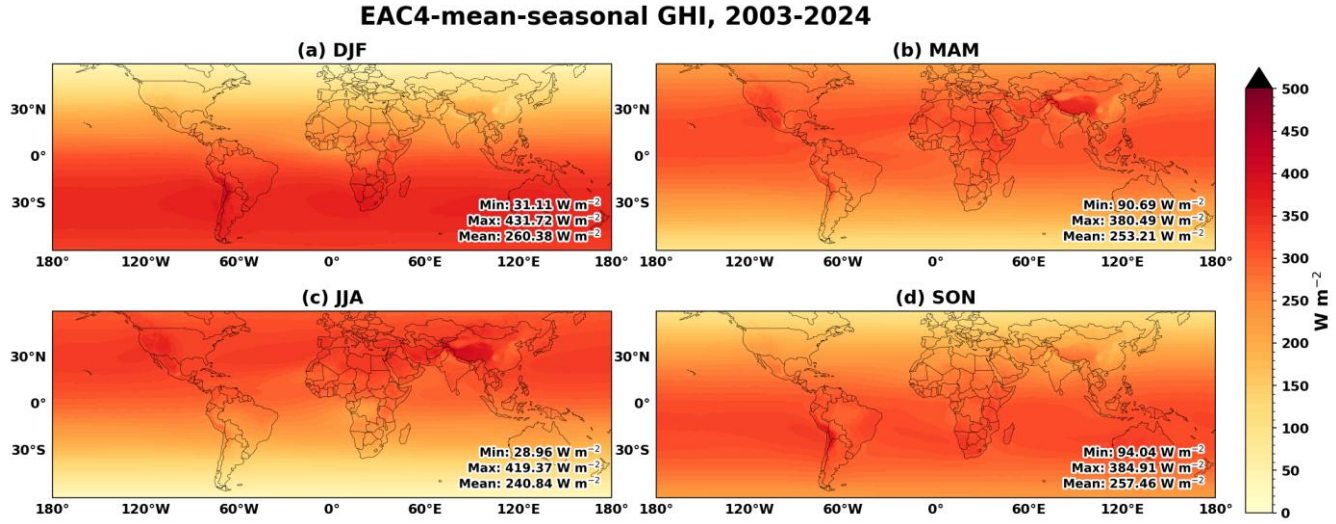


Figure S3: Spatial distribution of the mean-seasonal global horizontal irradiance (GHI) for the period 2003–2024. Panels (a) DJF, (b) MAM, (c) JJA, and (d) SON show the mean-seasonal GHI expressed in W m⁻².

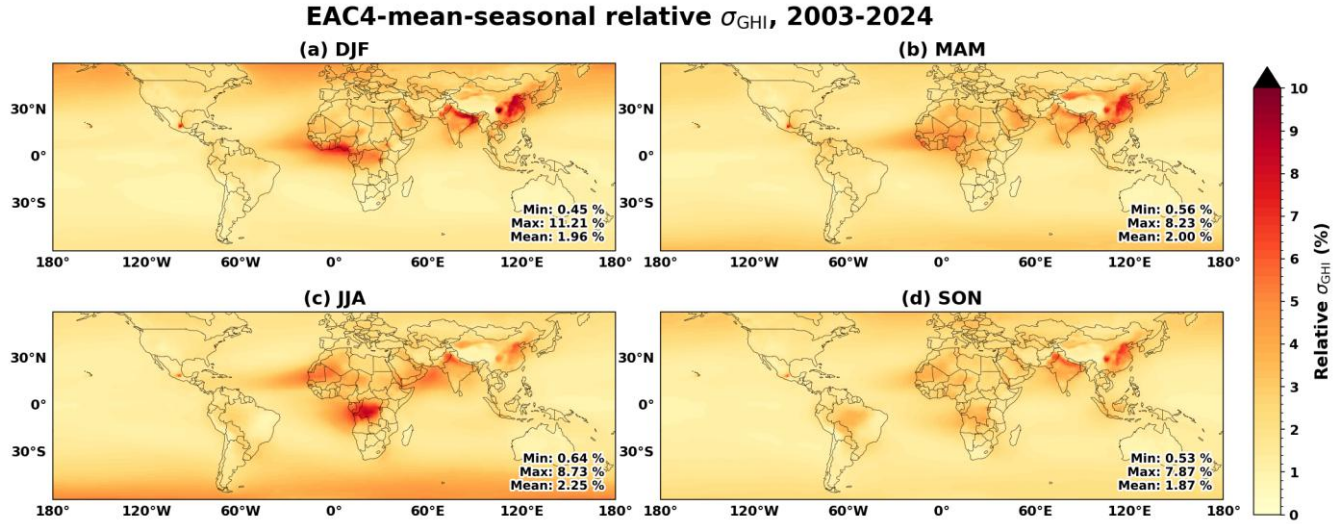


Figure S4: Spatial distribution of the mean-seasonal relative uncertainty of GHI (σ_{GHI}) for the period 2003–2024. Panels (a) DJF, (b) MAM, (c) JJA, and (d) SON show the mean-seasonal relative uncertainty of GHI (%).

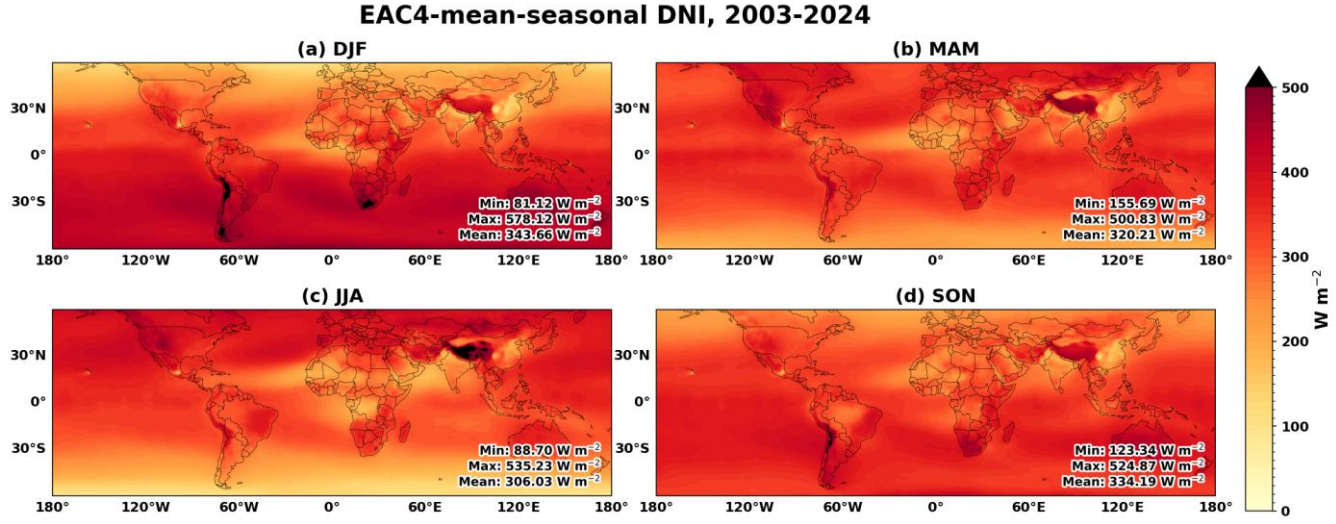


Figure S5: Spatial distribution of the mean-seasonal direct normal irradiance (DNI) for the period 2003–2024. Panels (a) DJF, (b) MAM, (c) JJA, and (d) SON show the mean-seasonal DNI expressed in W m⁻².

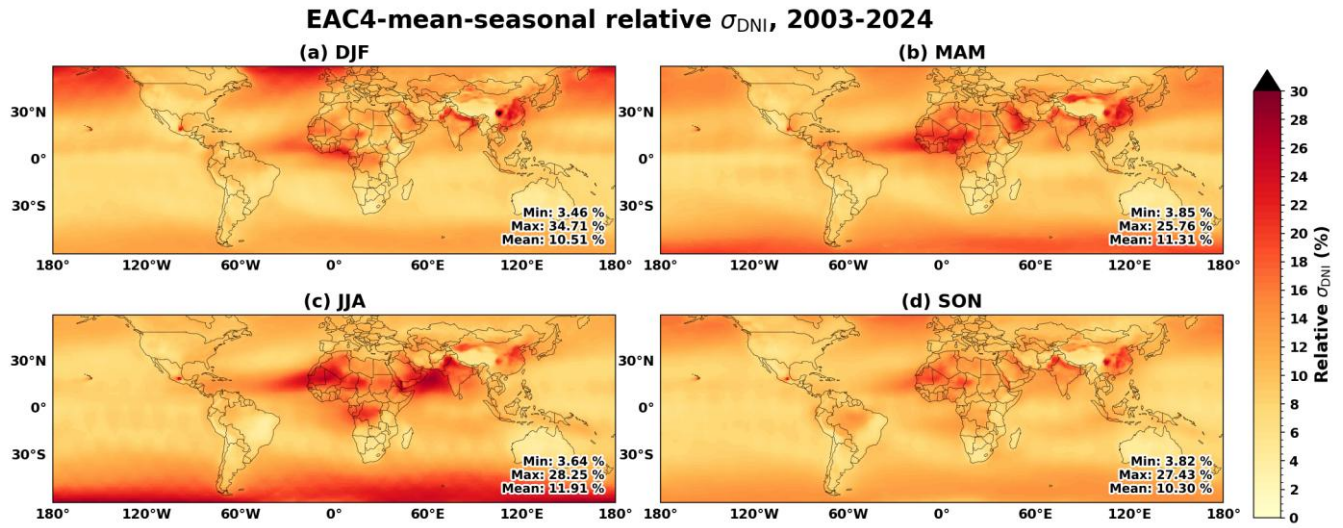


Figure S6: Spatial distribution of the mean-seasonal relative uncertainty of DNI (σ_{DNI}) for the period 2003–2024. Panels (a) DJF, (b) MAM, (c) JJA, and (d) SON show the mean-seasonal relative uncertainty of DNI (%).

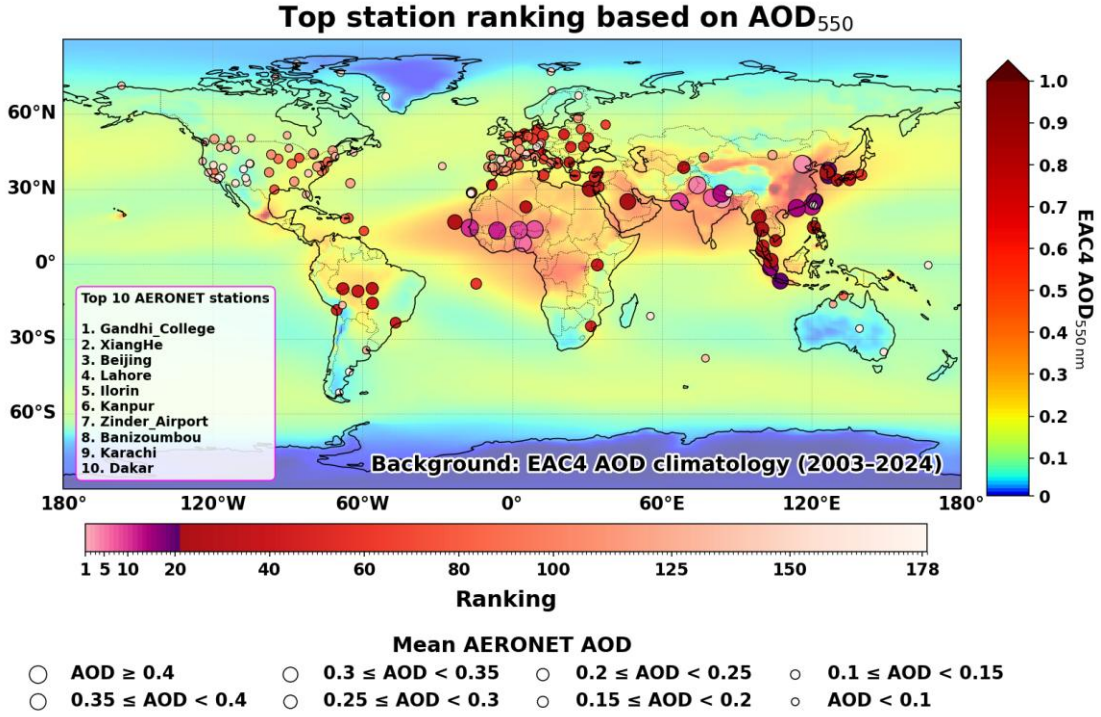


Figure S7: Global distribution and ranking of the 178 AERONET stations used in the present analysis based on their long-term mean AERONET AOD at 550 nm during the 2003–2024 period. The colored background represents the annual mean EAC4 AOD climatology at 550 nm for the same period. Marker colors indicate the ranking position of each station, while marker sizes correspond to different ranges of mean AERONET AOD.

Table S1: Geographical characteristics and mean aerosol optical depth at 550 nm (AOD_{550}) of the ten AERONET stations with the highest mean AOD_{550} values over the period 2003–2024 (based on AERONET). Stations are ranked in descending order of mean AOD_{550}. Latitude, longitude, and elevation are provided for each station.

Rank	Station	Latitude (°)	Longitude (°)	Elevation (m)	Mean AOD550
1	Gandhi_College	25.87	84.12	60	0.653
2	XiangHe	39.75	116.96	36	0.643
3	Beijing	39.97	116.38	92	0.635
4	Lahore	31.54	74.32	270	0.625
5	Ilorin	8.32	4.34	350	0.595
6	Kanpur	26.51	80.23	123	0.591
7	Zinder_Airport	13.77	8.99	456	0.493
8	Banizoumbou	13.54	2.66	250	0.472
9	Karachi	24.87	67.03	49	0.449
10	Dakar	14.39	-16.95	0	0.423

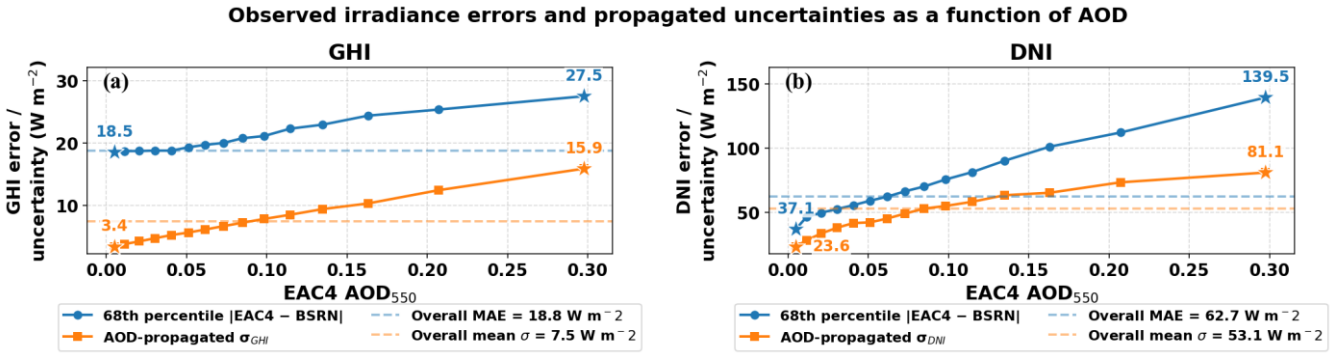


Figure S8: Observed clear-sky irradiance errors and AOD-propagated uncertainties as a function of EAC4 AOD_{550} for (a) GHI and (b) DNI. Collocations were divided into 15 equal-population bins according to EAC4 AOD_{550}. The 68th percentile of the absolute EAC4–BSRN difference (blue) and the median AOD-propagated irradiance uncertainty (orange) are shown for each bin. Dashed horizontal lines indicate the overall mean absolute error (MAE) and mean propagated uncertainty across all collocations, while stars highlight the values in the lowest- and highest-AOD bins.